scientific reports

Check for updates

OPEN

The diagnostic value of two-dimensional shear-wave elastography in identifying malignant lesions in lymph nodes: a prospective study

Jing Chen[1,2,3,4], Yao Deng[1,2,3,4], Jiajia Xiong[1,2,3], WenQu Li[1,2,3], Gongqun Shang[1,2,3], Hui Li[1,2,3], Yu Wu[1,2,3,5]✉ & Xiaojuan Qin[1,2,3,5]✉

This study evaluates the diagnostic performance of two-dimensional shear wave elastography (2D-SWE) in differentiating between benign, metastatic lymph nodes (LNs) and lymphomas. From May 2022 to February 2023, a total of 137 patients who presented with unexplained LN enlargement were examined at the Ultrasound Medical Department of Union Hospital of Huazhong University of Science and Technology. The conventional ultrasound recorded the location, longitudinal diameter, transverse diameter, L/T ratio, blood supply mode, lymphatic hilum and 2D-SWE calculated the average elasticity (E) of LN. Histopathology was the diagnostic gold standard. A total of 124 patients with 159 superficial LNs were included (32 benign, 70 metastatic, 57 lymphoma). Malignant LNs had significantly higher E values than benign ones (49.38 ± 29.96 kPa vs. 25.00 ± 14.42 kPa, $P < 0.001$). When E > 25.46 kPa, the AUC, sensitivity, specificity, PPV, NPV and accuracy were 0.807, 0.787, 0.750, 0.926, 0.471 and 0.780, respectively, in identifying malignant LNs. For distinguishing benign LNs from lymphoma, the E cutoff was 25.03 kPa, with the AUC, sensitivity, specificity, PPV, NPV and accuracy of 0.727, 0.754, 0.719, 0.827, 0.622 and 0.742, respectively. To differentiate benign from metastatic LNs, an E cutoff of 36.97 kPa yielded an AUC, sensitivity, specificity, PPV, NPV and accuracy of 0.872, 0.757, 0.875, 0.930, 0.622 and 0.794, respectively. Comparing lymphoma and metastatic LNs, the E cutoff was 42.57 kPa. And the AUC, sensitivity, specificity, PPV, NPV and accuracy were 0.787, 0.700, 0.860, 0.860, 0.700 and 0.772, respectively. 2D-SWE parameter (the average elasticity) can effectively evaluate benign, metastatic LNs and lymphoma, which provides valuable information for preoperative evaluation of superficial LNs.

Keywords Ultrasound, Shear-wave elastography, Superficial lymph nodes, Differential diagnosis

Abbreviations

2D-SWE	Two-dimensional shear wave elastography
LN	Lymph node
E	Elasticity
US	Ultrasound
USE	Ultrasound elastography
L/T	Longitudinal to transverse
ROI	Region of interest
ROC	Receiver operating characteristic
AUC	Area under the curve
PPV	Positive predictive value

[1]Department of Ultrasound Medicine, Union Hospital, Tongji Medical College, Huazhong University of Science and Technology, Wuhan 430022, China. [2]Hubei Province Clinical Research Center for Medical Imaging, Wuhan 430022, China. [3]Hubei Province Key Laboratory of Molecular Imaging, Wuhan 430022, China. [4]Jing Chen and Yao Deng those have contributed equally and are co-first authors. [5]Yu Wu and Xiaojuan Qin those have contributed equally and are co-corresponding authors. ✉email: Poyueng@126.com; qinxiaojuan11@hust.edu.cn

NPV	Negative predictive value
DAMP	Damage-associated molecular pattern

Superficial lymph node (LN) abnormalities may result from a diverse range of causes, including both benign and malignant lesions. Benign LN lesions are associated with a favorable prognosis, whereas malignant lesions have a poor prognosis. Given the significant differences in prognosis and treatment, accurate differentiation between benign and malignant lesions is crucial for guiding treatment decisions and evaluating prognosis. Although histological pathology remains the gold standard for diagnosing benign and malignant LN lesions, the invasive nature of this approach makes it difficult for some patients to accept. Therefore, it is essential to utilize reliable techniques to assist in the identification of superficial LNs to avoid unnecessary biopsies.

Current imaging techniques for evaluating LNs include ultrasound (US), computed tomography (CT), magnetic resonance (MR) imaging, and positron emission tomography (PET-CT). In CT and MR imaging, the determination of LN malignancy is primarily based on size criteria. However, up to 30% of LNs less than 5 mm have been shown to have malignant infiltration in lung, esophageal, gastric, pancreatic, and rectal cancers[1]. 18 F-fludeoxyglucose–positron emission tomography/computed tomography (FDG-PET/CT) is increasingly available and used in cancer staging; however, meta-analyses also indicate insufficient sensitivity for the detection of early LN metastasis[2,3]. US is the preferred tool for evaluating LNs due to its safety, convenience, and relatively low cost. Conventional US is primarily based on the size, morphological structure, and blood flow characteristics of LNs to distinguish between benign and malignant lesions[4,5]. However, there is some overlap between these ultrasonic features in benign and malignant LNs, which leads to unsatisfactory sensitivity and specificity for the diagnosis of superficial LNs [6–8]. Therefore, there is an urgent need to develop new technologies and methods to improve the differentiation ability of benign and malignant LN lesions.

In recent years, ultrasound elastography (USE) techniques have received increasing attention for their non-invasive assessment of tissue mechanical properties, with a primary focus on clinical diagnosis of soft tissue organ diseases. Compared to anatomical images, elastography can provide auxiliary diagnostic information on tissue mechanics. Many studies have shown that elastic imaging can effectively differentiate benign and malignant lesions, and it has been widely used in thyroid, breast, liver, and other organs[9–13]. 2D-SWE is currently the newest SWI method. Acoustic Radiation Force Impulse (ARFI) strain imaging employs brief acoustic radiation force pulses to induce local tissue displacement and subsequently monitors the tissue response within the targeted region[14]. Point Shear Wave Elastography (pSWE) utilizes acoustic radiation force to generate shear waves at a single point, measuring the shear wave speed at that location to estimate tissue stiffness[15]. However, both methods are limited to single-point or small localized assessments, requiring multiple excitations and measurements to evaluate larger areas, which increases operational complexity. In contrast, 2D-SWE induces shear waves at multiple points and tracks their propagation speed or Young's modulus (E) in real time, generating a comprehensive two-dimensional elasticity map that encompasses the entire region[15]. The capability to provide real-time, wide-area coverage makes 2D-SWE particularly advantageous for assessing larger areas or complex lesions. Several studies have verified the diagnostic value of 2D-SWE for benign and malignant LNs. However, malignant LN lesions include metastatic LNs and lymphoma, and the clinical treatment and management principles of the two are inconsistent. Therefore, effective identification of both is crucial. The purpose of this study was to compare the differential diagnostic value of 2D-SWE in benign, metastatic LNs, and lymphoma.

Methods

Patients

From May 2022 to February 2023, patients who presented to the Ultrasound Medical Department of Union Hospital of Huazhong University of Science and Technology for examination due to unexplained LN enlargement in the neck, axilla, and groin were included. The inclusive criteria were as follows: (1) Transverse axis > 5 mm and longitudinal-to-transverse ratio (L/T ratio) < 2, or transverse axis > 10 mm[16]; (2) LNs were evaluated by US and 2D-SWE imaging before biopsy; and (3) The patient underwent pathological examination.

Exclusion criteria: (1) History of malignant tumor or tuberculosis; (2) LNs without pathological results or with unclear pathological results; (3) LNs with fluid parts; (4) LNs with unsatisfactory 2D-SWE images. This study was approved by the Ethics Committee of Union Hospital Affiliated to Tongji Medical College of Huazhong University of Science and Technology (Ethics approval ID: UHCT-IEC-SOP-016-03-01), and informed consent was obtained from all patients. We confirm that all methods were performed in accordance with relevant guidelines and regulations.

Ultrasound imaging

An ultrasound examination was conducted by an ultrasound doctor with 10 years of experience. The conventional US data and 2D-SWE images were captured separately using LOGIQ E9 (GE, USA) with linear probes L16-5 and 9L4. Conventional ultrasound was performed using the probe L16-5, with the gain set to 40–50 and the frequency set to 11–13 MHz. The location, longitudinal diameter, transverse diameter, structure, and blood supply of the LNs were recorded. Doppler ultrasound was performed using standardized Doppler parameters, set to high sensitivity and a low wall filter to detect blood vessels with weaker blood flow (frequency: 6.3–7.5 MHz; gain: 18.5–22.5; scale: 5–6 cm/s; pulse repetition frequency: 1.0–1.6 kHz). The Color Doppler pattern of LNs is classified into four types: (1) hilar or central: blood flow signals branching from the center or exhibiting a radial branching pattern (even if starting from the periphery); (2) peripheral: blood flow signals along the periphery of the LN; (3) mixed: both peripheral and central blood flow signals are present; (4) no blood flow: no blood flow signals within the LN.

After conventional ultrasound determined the target LN, 2D-SWE was performed using the linear probe 9L4. The probe was gently placed vertically on the surface of the skin over the target LN, and the appropriate region of interest (ROI) was adjusted to surround the entire LN. The gain was then adjusted to over 95. The probe was stabilized, and the patient was asked to hold their breath while the ultrasound probe was held still over the target LN without pressure for 10 s to ensure stable color area coverage, after which the image was saved. The ROI coverage rate was greater than 95%. For quantitative assessment, the outline of the target LN was drawn manually, and the instrument software automatically calculated the average E of the ROI. Each LN was measured three times, and the mean value was calculated.

Pathological examination

Pathological diagnosis was obtained by ultrasound-guided nodal puncture or resection. Tissue biopsy, including pathological section and immunohistochemical examination, was performed.

Statistical analysis

The data were analyzed using SPSS software (version 27.0.1). Qualitative variables were expressed in numbers and percentages, while quantitative variables were expressed in mean ± standard deviation ($\bar{x} \pm s$). The chi-square test and Fisher's exact test were used to compare proportions, and one-way ANOVA was used to compare mean values that followed a normal distribution. Bonferroni and Tamhane T2 tests were used to compare independent groups. Confidence intervals (CI) were used as the 95% CI for exact binomial bilateral. Sensitivity, specificity, positive predictive value (PPV), negative predictive value (NPV) and accuracy were calculated. The receiver operating characteristic (ROC) curve was used to evaluate the area under the curve (AUC) of the mean value of E. The correlation between E value and LN size was assessed using the nonparametric Spearman's rank correlation coefficient (R). $P < 0.05$ was considered statistically significant. The measurement of E value was conducted by two different doctors using a blind method, and we tested the reliability within and between observers. A Cronbach alpha of more than 0.7 was considered reliable.

Results

A total of 174 LNs from 137 patients underwent 2D-SWE and biopsy. 13 patients with 15 LNs were excluded due to lack or unclear pathological diagnosis ($n = 11$), LNs with fluid parts ($n = 2$), or unsatisfactory 2D-SWE images ($n = 2$). Finally, 159 LNs from 124 patients were enrolled in this study. The flow chart is presented in Fig. 1. 20.1% of LNs were benign LN lesions, and the remaining 79.9% were malignant LN lesions. The general demographic characteristics are presented in Table 1.

Differentiation between benign and malignant LNs

Table 2 presents the conventional US and 2D-SWE characteristics of all LNs. The results showed significant differences in the transverse axis, L/T ratio, lymphatic hilum, Color Doppler pattern, and 2D-SWE parameter between benign and malignant LNs ($p < 0.05$). However, there was no statistical difference in the longitudinal axis. Figure 2 shows the 2D-SWE and grayscale US images.

An ROC curve was constructed to determine the diagnostic performance of 2D-SWE parameters for benign and malignant LNs. Specifically, the cut-off value of E was 25.46 kPa, and the AUC, sensitivity, specificity, PPV, NPV and accuracy were 0.807, 0.787, 0.750, 0.926, 0.471 and 0.780, respectively. The ROC curve is shown in Fig. 3.

Differentiation between benign LNs, lymphoma and metastatic LNs

Table 3 presents the conventional US and 2D-SWE characteristics of all LNs. The results showed significant differences in the transverse axis, L/T ratio, lymphatic hilum, Color Doppler pattern, and 2D-SWE parameter

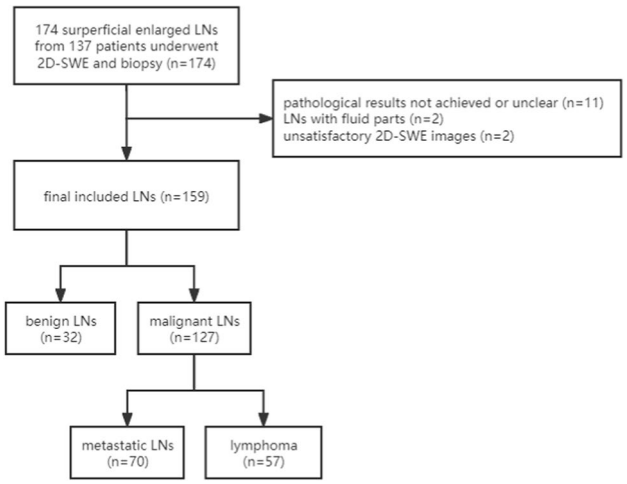

Fig. 1. Flowchart of the study. LNs, lymph nodes; 2D-SWE, two-dimensional shear wave elastography.

Characteristic	
Age (years) Mean ± SD	54.6 ± 14.2
Gender	
Male (N/%)	62 /50.0%
Female (N/%)	62 /50.0%
Localization	
Neck (N/%)	90 /56.6%
Axilla (N/%)	43 /27.0%
Inguinal (N/%)	26 /16.4%
Benign LNs	
Reactive hyperplasia (N/%)	13 /8.2%
Granulomatous lesions or tuberculosis (N/%)	10 /6.3%
Non-specific LNs (N/%)	9 /5.7%
Malignant LNs	
Lymphoma (N)	**57**
Hodgkin's lymphoma (N/%)	12 /7.5%
Mixed cellularity (N/%)	5 /3.1%
Nodular sclerosis (N/%)	2 /1.3%
Lymphocyte-rich (N/%)	2 /1.3%
Unclassified (N/%)	3 /1.9%
Non-Hodgkin's lymphoma (N/%)	45 /28.3%
Follicular lymphoma	13 /8.2%
Diffuse large B-cell lymphoma	9 /5.7%
Angioimmunblastic T-cell lymphoma	6 /3.8%
Small lymphocytic lymphoma	6 /3.8%
NK/T cell lymphoma	3 /1.9%
Marginal zone lymphoma	2 /1.3%
Peripheral T-cell lymphoma	2 /1.3%
T cell lymphoblastic lymphoma	1 /0.6%
Anaplastic large cell lymphoma	1 /0.6%
Mantle cell lymphoma	1 /0.6%
Unclassified	1 /0.6%
Metastatic LNs (N)	**70**
Lung cancer (N/%)	32 /20.1%
Breast cancer (N/%)	19 /11.9%
Others (N/%)	19 /11.9%

Table 1. The general demographic characteristics. SD, standard deviation.

between benign LNs, lymphoma and metastatic LNs ($p < 0.05$). However, there was no statistical difference in the longitudinal axis between benign and metastatic LNs.

We compared the three groups of benign LNs, lymphoma, and metastatic LNs in pairs and constructed ROC curves to determine the diagnostic performance of 2D-SWE parameters in differentiating among them. The ROC curve is shown in Fig. 4.

Table 4 shows the cut-off value, the AUC, sensitivity, specificity and accuracy for classifying each type of LN.

Relationship between the E value and LN size

Analysis of all LN samples revealed no significant correlation between the longitudinal axis of the LNs and the E value (Fig. 5A, $R = 0.033$, $P = 0.682$). A very weak correlation was observed between the transverse axis of the LNs and the E value (Fig. 5B, $R = 0.189$, $P = 0.017$). Although this correlation reached statistical significance ($P < 0.05$), the effect size ($R = 0.189$) is considered too small to be practical clinical significance.

Upon grouping the samples, within the benign LN group, no significant correlations were found between the E value and either the longitudinal axis ($R = 0.558$, $P = 0.107$) or the transverse axis ($R = 0.338$, $P = 0.059$) of the LNs. Similarly, in the lymphoma group, no significant correlations were observed between the E value and either the longitudinal axis (R=-0.13, $P = 0.336$) or the transverse axis (R=-0.023, $P = 0.863$) of the LNs. In the metastatic LN group, the E value also did not show a significant correlation with either the longitudinal axis ($R = 0.227$, $P = 0.059$) or the transverse axis ($R = 0.208$, $P = 0.085$) of the LNs.

	Benign ($n=32$)	Malignant ($n=127$)	P value
Size (mm)			
Longitudinal axis	20.52 ± 8.63	23.94 ± 9.51	0.066
Transverse axis*	10.64 ± 3.23	14.24 ± 4.94	< 0.001
L/T ratio* (N/%)			
≥2	12 /37.5%	21 /16.5%	
<2	20 /62.5%	106 /83.5%	0.009
Lymphatic hilum* (N/%)			
Present	17 /53.1%	20 /15.7%	
Absent	15 /46.9%	107 /84.3%	< 0.001
Color Doppler pattern* (N/%)			
Hilar or central	17 /53.1%	26 /20.5%	
Peripheral	1 /3.1%	24 /18.9%	
Mixed	10 /31.3%	72 /56.7%	
No blood flow	4 /12.5%	5 /3.9%	< 0.001
2D-SWE parameter			
E (kPa)*	25.00 ± 14.42	49.38 ± 29.96	< 0.001

Table 2. Conventional US and 2D-SWE characteristics of benign and malignant LNs. *Values are presented as the mean ± standard deviation or percentage, respectively.

Intra- and interobserver reliabilities of the 2D-SWE measurements

The consistency of the 2D-SWE measurements in our study is very high. The intra- and interobserver reliability were 0.969 (observer 1), 0.968 (observer 2), and 0.999 (interobserver), respectively, calculated using Cronbach alpha.

Discussion

The differentiation of abnormal LNs in benign conditions such as infection or inflammation from malignant conditions such as metastatic disease or primary malignancies such as lymphoma is clinically significant. Conventional US mainly relies on anatomical morphological changes or vascular patterns[5,8], which may overlap in different LN lesions. USE, which takes advantage of the changed elasticity of soft tissues resulting from specific pathological or physiological processes[17], provides complementary information to conventional US and can effectively distinguish between benign and malignant lesions[15]. The results of this study showed that 2D-SWE had good diagnostic performance in assessing LN status, and E could be used as an effective tool for preoperative evaluation of superficial LNs.

In our study, we observed that malignant LNs were larger than benign LNs, and the proportion of L/T ratio < 2 was higher. This can be explained by the presence of lymphocyte accumulation and lymphatic sinus growth in malignant LNs, which tend to be larger in size compared to benign LNs[18]. Furthermore, malignant infiltration typically occurs in the cortex[19], thus changing the structure of the LNs and making the LN shape change from oval to round. Additionally, the probability of disappearance of the lymphatic hilum is higher in malignant LNs. The lymphatic hilum represents the collecting sinus of a normal LN[20]. The absence of the lymphatic hilum may indicate that it has been erased by infiltrating tumor cells. The Color Doppler patterns of benign and malignant LNs also differ, with the most common pattern in benign LNs being hilar or central, while in malignant LNs, the proportion of mixed and peripheral patterns is increased. These vascular differences in malignant LNs are thought to be caused by additional angiogenesis of infiltrating tumor cells[21]. However, there is significant variation in the vascular patterns of malignant LNs. Bialek et al. reported that blood flow in lymphomas can exhibit both metastatic and benign patterns[5]. Furthermore, the vascular patterns in LNs are influenced by the equipment used and the operator's technique[22]. Relying solely on blood flow is inadequate for distinguishing between benign and malignant LNs.

USE has been proven to be helpful in distinguishing benign from malignant LNs through stiffness assessment. In this study, we observed higher E values in malignant LNs compared to benign LNs, similar to previous studies[23]. This can be explained by specific histologic features of different LNs. Invasive malignant tumors may lead to deposition of extracellular matrix and cross-linked collagen, ultimately affecting tissue stiffness[24,25]. Rizwan et al. also observed a significant increase in collagen density in metastatic LNs[26].

In this study, the average E values of the lymphoma group and the metastatic LNs were 32.79 kPa and 62.89 kPa, respectively. These values are somewhat different from previous reports[27,28]. Guan et al. pointed out that the E value of neck metastatic LNs was 23.48 kPa[27], which was significantly lower than our study. This discrepancy may be due to their focus on small cervical LNs (0.5 cm ≤ maximum diameter < 1 cm) associated with nasopharyngeal carcinoma. Their results indicated no significant differences between benign and metastatic LNs when assessed using conventional ultrasound. Therefore, the metastatic LNs in their study may still be in an early stage, likely indicating micrometastasis, which typically shows less stromal reaction[29]. This reduced reaction is a key factor contributing to the increased stiffness observed in metastatic LNs[30]. Moreover, our study

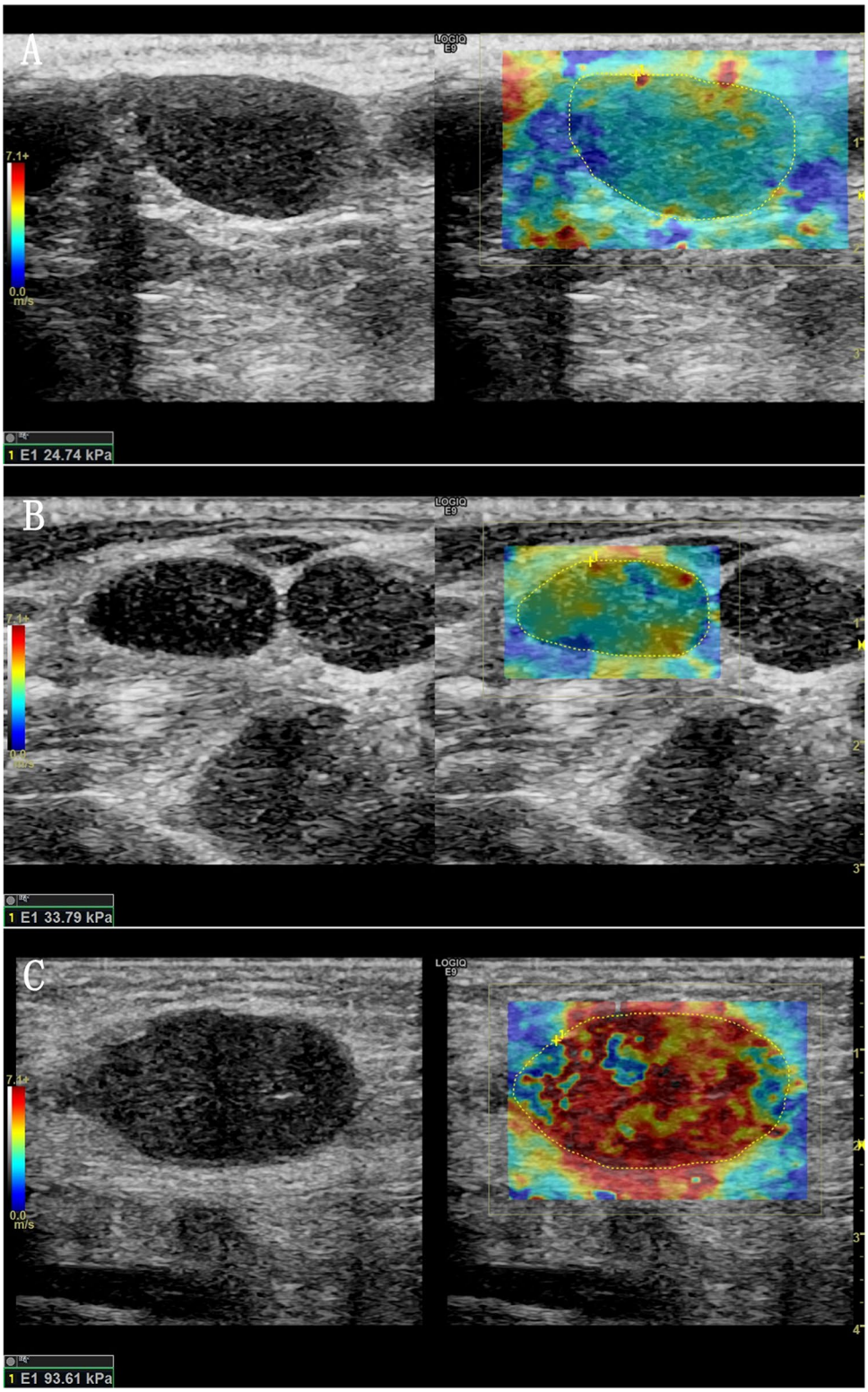

Fig. 2. The 2D-SWE images of LNs, with pathological results proven reactive LN (**A**), lymphoma (**B**) and metastatic LN of breast cancer (**C**), respectively.

included a wider variety of benign LNs, such as those with reactive hyperplasia and tuberculosis, which may explain the higher stiffness values observed in our benign group compared to theirs.

However, Chae et al. pointed out that the average E of cervical metastatic LNs was 94.87 kPa[28], which was higher than that of our study. This may be because they placed the ROI on the stiffest area, whereas in our study, the ROI encompasses the entire target LN. We believe that measuring only the stiffest part does not accurately

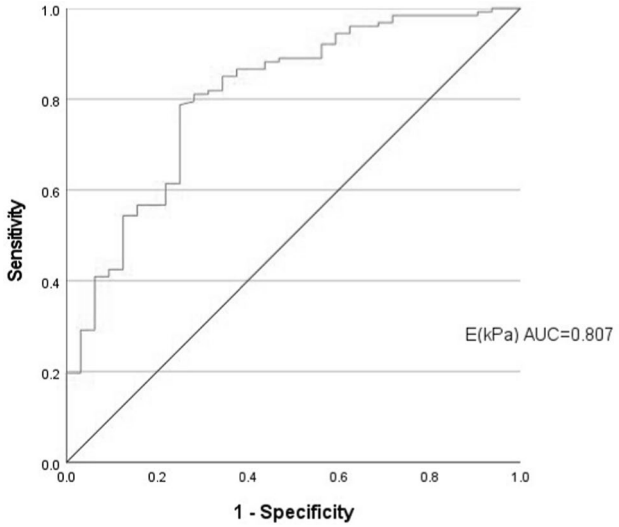

Fig. 3. ROC curves of E value for differentiating between benign and malignant LNs.

	Benign ($n=32$)	Lymphoma ($n=57$)	Metastatic ($n=70$)	*P* value
Size (mm)				
Longitudinal axis	20.52 ± 8.63	27.19 ± 10.33	21.29 ± 7.93	†=0.003*, ††=1, †††<0.001*
Transverse axis	10.64 ± 3.23	15.62 ± 5.38	13.12 ± 4.26	†<0.001*, ††=0.034*, †††=0.007*
L/T ratio (N/%)				
≥2	12 /37.5%	12 /21.1%	9 /12.9%	
<2	20 /62.5%	45 /78.9%	61 /87.1%	<0.05*
Lymphatic hilum (N/%)				
Present	17 /53.1%	15 /26.3%	5 /7.1%	
Absent	15 /46.9%	42 /73.7%	65 /92.9%	<0.05*
Color Doppler pattern (N/%)				
Hilar or central	17 /53.1%	12 /21.1%	14 /20.0%	
Peripheral	1 /3.1%	5 /8.8%	19 /27.1%	
Mixed	10 /31.3%	38 /66.7%	34 /48.6%	
No blood flow	4 /12.5%	2 /3.5%	3 /4.3%	<0.05*
2D-SWE parameter				
E (kPa)	25.00 ± 14.42	32.79 ± 12.26	62.89 ± 33.23	†=0.038*, ††,†††<0.001*

Table 3. Conventional US and 2D-SWE characteristics of benign LNs, lymphoma and metastatic LNs. *Values are presented as the mean ± standard deviation or percentage, respectively. †Statistically significant difference between benign and lymphoma. †† Statistically significant difference between benign and metastatic. ††† Statistically significant difference between lymphoma and metastatic.

represent the overall state of the LN, as even in normal LNs, the elasticity values are heterogeneous. For example, lymphocyte-rich mantle zones and germinal centers have higher elasticity values[30]. In metastatic LNs, areas with desmoplastic reactions might show the highest elasticity values, allowing for differentiation from benign LNs. However, in lymphomas, there are no specific areas with particularly high elasticity values, as the normal architecture is completely lost and replaced by densely monotonous lymphoma cells[30]. Therefore, it presents as a more uniform phenomenon with overall higher elasticity values. In reactive hyperplastic LNs, areas of follicular hyperplasia are also present, leading to locally elevated elasticity values; however, these changes are typically restricted to the subcortical region. Consequently, relying solely on the maximal elasticity value may complicate the differentiation between benign LNs and lymphoma. In contrast, employing the average elasticity value is more effective in distinguishing between these conditions. Furthermore, our ROI encompasses the entire LN, thereby diminishing operator dependency and enhancing the reproducibility of stiffness measurements. The results of our study also showed a good correlation between multiple measurements by the same observer and different observers. However, this method may reduce the sensitivity to changes in stiffness. In addition, different devices may lead to different 2D-SWE values[31].

Although they are all malignant tumors, the E values in metastatic LNs were significantly greater than those in lymphoma, consistent with previous research results[28]. This may be related to the pathological differences

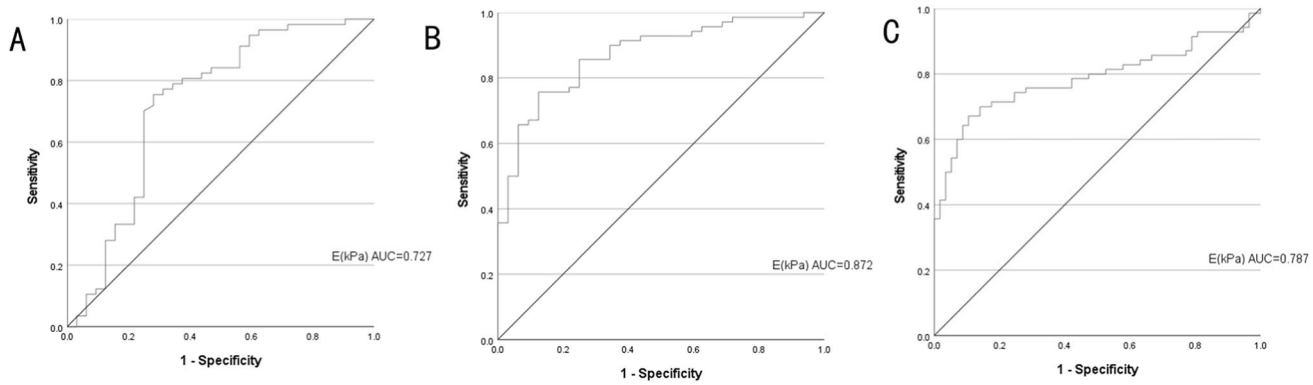

Fig. 4. ROC curves of E value for differentiating between benign and lymphoma (**A**), benign and metastatic LNs (**B**), lymphoma and metastatic LNs (C).

	Cut-off (E, kPa)	AUC (95% CI)	Sensitivity	Specificity	PPV	NPV	Accuracy	*P* value
Benign and lymphoma	25.03	0.727 (0.606–0.849)	0.754	0.719	0.827	0.622	0.742	< 0.001
Benign and metastatic	36.97	0.872 (0.802–0.942)	0.757	0.875	0.930	0.622	0.794	< 0.001
Lymphoma and metastatic	42.57	0.787 (0.705–0.868)	0.700	0.860	0.860	0.700	0.772	< 0.001

Table 4. Diagnostic performances of 2D-SWE for differentiating between benign LNs, lymphoma and metastatic LNs. AUC, area under the ROC curve; CI, confidence intervals; PPV, positive predictive value; NPV, negative predictive value; kPa, kilopascals.

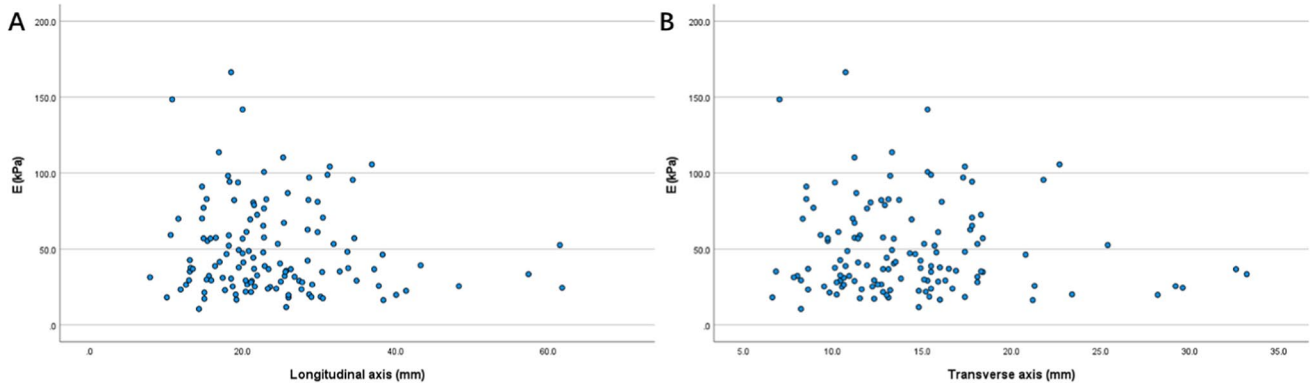

Fig. 5. Relationship between the E value and the longitudinal axis (**A**) or the transverse axis (**B**).

between them. In metastatic LNs, tumor cells and stromal cells undergo proliferation and cornification, producing a large amount of keratins and fibrin. However, lymphoma has proliferation characterized by less fibrotic changes (promoting connective tissue proliferation)[30]. Therefore, compared to metastatic LNs, their stiffness is lower. Compared to benign LNs, lymphoma exhibits greater stiffness. This may be attributed to the pronounced follicular hyperplasia in lymphoma, which results in a higher cellular nuclear density[30]. As previously noted, reactive LNs also show follicular hyperplasia, but it is typically restricted to the subcortical areas. On the other hand, follicular lymphoma has a more uniform distribution throughout the LN parenchyma[32].

In this study, the cutoff of E value for distinguishing benign LNs from malignant LNs was 25.46 kPa, and the AUC, sensitivity, specificity, PPV, NPV and accuracy were 0.807, 0.787, 0.750, 0.926, 0.471 and 0.780, respectively. This result is similar to the study of Luo et al.[33]. Luo et al. reported that the cutoff of E value for distinguishing benign and malignant LNs was 23.2 kPa[33]. However, our results are somewhat inconsistent with those of Chami et al., who reported a lower critical value of 15.2 kPa to distinguish malignant LNs from benign LNs[34]. The difference in sample characteristics between the two studies may explain the difference between the two results. In the study of Chami et al., some infectious diseases such as abscesses and tuberculosis were excluded[34], while our study includes tuberculosis or granulomatous lesions. In granulomatous lymphadenitis, particularly during the late phase, the increase of collagen fibers results in fibrosis, which subsequently increases the stiffness of the LNs[35].

In addition, Sun et al. reported that the cutoff of E value for distinguishing benign and malignant LNs was 42 kPa, the sensitivity was 0.927, and the specificity was 0.975[23], much higher than our study. This difference may stem from the higher proportion of metastatic LNs in their malignant LN group, which is 79.0%, compared to 55.1% in our group. The presence of lymphoma reduces the overall elasticity in our malignant LN group. Of course, this difference may also be related to the method of ROI placement. Taking 25.46 kPa as the cutoff value, we found that the E value of 8 benign LNs was higher than the cutoff value, including 4 cases of tuberculosis or granulomatous lesions, 3 cases of reactive hyperplasia, and 1 case of non-specific LN. The most characteristic pathological features of tuberculosis are epithelioid granulomas and caseous necrosis[36]. As noted earlier, fibrosis in granulomatous lesions contributes to increased LN stiffness. Some reactive LNs may also exhibit granulomas or necrosis[37]. In our study, despite the exclusion of cystic necrosis, we found that coagulation necrosis accompanied by cell-rich debris was associated with significantly elevated tissue stiffness. We hypothesize that during the advanced stages of coagulation necrosis, necroptosis leads to the release of damage-associated molecular patterns (DAMPs). These DAMPs may initiate immune responses, promote fibroblast activation, and increase extracellular matrix deposition, thereby contributing to the observed increase in tissue stiffness[38]. This could be one of the factors contributing to our elevated false positive rate.

We also compared the differences among the benign LNs, lymphoma and metastatic LNs. The diagnostic performance was found to be best in the benign and metastatic LNs, while the performance of the benign LNs and lymphoma was relatively poorer. This discrepancy may stem from the fact that both reactive hyperplasia of LNs and lymphoma are primarily proliferative changes, leading to less fibrosis and a smaller difference in elastic values[37]. In future studies, we can investigate the diagnostic performance of combining conventional ultrasound, color Doppler, contrast-enhanced ultrasound, and elastography. In the study of Bayramoglu et al., the cutoff value of E for distinguishing lymphoma from lymphadenitis was found to be 17 kPa, which is lower than our findings[39]. This difference may be attributed to their selection of inflammatory LNs based on clinical manifestations such as fever and laboratory parameters, including white blood cell count, C-reactive protein, and sedimentation rate, which predominantly indicated acute inflammation in most cases. Acute lymphadenitis is primarily characterized by the infiltration of inflammatory cells, whereas chronic lymphadenitis may exhibit fibrosis and granuloma formation that significantly elevate the elastic value of the LNs[32]. In our study, we observed that the PPV was higher while the NPV was lower. This may be due to our approach of measuring the average elasticity of the entire LN, which could compromise sensitivity and hinder early detection of elastic changes. However, this method may be more appropriate for screening high-risk populations. For instance, if a patient has a history of tumors and the measured elasticity value is elevated, our diagnostic confidence can be significantly enhanced.

We also investigated the potential correlation between the E value and LN size. However, neither the analysis of all LN samples nor the subgroup analyses revealed a significant correlation between these variables. We hypothesize that this may be attributed to the limited sample size of our LNs and the non-normal distribution of the selected LN sizes. Furthermore, the substantial variability in pathological types across the LN groups may have partially influenced the results.

Our study has several limitations. Firstly, the sample size is small, particularly the number of benign LNs is not as extensive as malignant LNs. Secondly, this study has a certain selection bias, particularly in benign LNs, the proportion of completely normal LNs is very small, mostly reactive hyperplasia, granulomatous LNs, etc. Furthermore, both lymphoma and metastatic LNs encompass a diverse array of pathological types; however, the number of cases for each subtype remains relatively limited, posing significant challenges in conducting detailed studies on specific pathological subtypes. In the subsequent phase of our investigation, we aim to expand the sample size of these specific pathological subtypes. Thirdly, due to the differences in the results of E values caused by different machines and different ROI placement methods, specific cut-off values may be limited in clinical practice of different institutions.

Conclusions

In conclusion, our study demonstrates that the stiffness of benign LNs, lymphoma, and metastatic LNs increases in turn. 2D-SWE is expected to be a promising imaging method for preoperative differentiation of the pathological properties of superficial LNs.

Data availability

The data that support the findings of this study are available on request from the corresponding author (qinxiaojuan11@hust.edu.cn).

Received: 25 August 2024; Accepted: 28 April 2025
Published online: 19 May 2025

References

1. Cui, X. W., Jenssen, C., Saftoiu, A., Ignee, A. & Dietrich, C. F. New ultrasound techniques for lymph node evaluation. *World J. Gastroenterol.* **19**, 4850–4860 (2013).
2. Dinnes, J. et al. MRI, or PET-CT for staging and re-staging of adults with cutaneous melanoma. *Cochrane Database Syst. Rev.* **7**, CD012806 (2019). Ultrasound, CT.
3. Zhang, X., Liu, Y., Luo, H. & Zhang, J. PET/CT and MRI for identifying axillary lymph node metastases in breast Cancer patients: systematic review and Meta-Analysis. *J. Magn. Reson. Imaging.* **52**, 1840–1851 (2020).
4. Zhang, X., Wang, L., Feng, N., Ni, T. & Tang, W. Reassessing the value of Contrast-Enhanced ultrasonography in differential diagnosis of cervical tuberculous lymphadenitis and lymph node metastasis of papillary thyroid carcinoma. *Front. Oncol.* **11**, 694449 (2021).

5. Bialek, E. J. et al. Vascular patterns in superficial lymphomatous lymph nodes: A detailed sonographic analysis(). *J. Ultrasound*. **10**, 128–134 (2007).
6. Suh, C. H., Choi, Y. J., Baek, J. H. & Lee, J. H. The diagnostic performance of shear wave elastography for malignant cervical lymph nodes: A systematic review and meta-analysis. *Eur. Radiol.* **27**, 222–230 (2017).
7. Leenhardt, L. et al. European thyroid association guidelines for cervical ultrasound scan and ultrasound-guided techniques in the postoperative management of patients with thyroid cancer. *Eur Thyroid J* 2, 147–159 (2013). (2013).
8. Ahuja, A. T., Ying, M., Ho, S. S. & Metreweli, C. Distribution of intranodal vessels in differentiating benign from metastatic neck nodes. *Clin. Radiol.* **56**, 197–201 (2001).
9. Swan, K. Z., Nielsen, V. E. & Bonnema, S. J. Evaluation of thyroid nodules by shear wave elastography: a review of current knowledge. *J. Endocrinol. Invest*. **44**, 2043–2056 (2021).
10. Gu, J. et al. Hybrid high-definition microvessel imaging/shear wave elastography improves breast lesion characterization. *Breast Cancer Res.* **24**, 16 (2022).
11. Deurdulian, C. et al. Assessment of fibrosis in liver transplant recipients: diagnostic performance of shear wave elastography (SWE) and correlation of SWE findings with biopsy results. *AJR Am. J. Roentgenol.* **213**, W264–W271 (2019).
12. Schulz, M. et al. Shear wave elastography and shear wave dispersion imaging in primary biliary cholangitis-a pilot study. *Quant. Imaging Med. Surg.* **12**, 1235–1242 (2022).
13. Kolb, M. et al. Shear wave elastography for assessment of muscular abnormalities related to systemic sclerosis. *Acad. Radiol.* **28**, 1118–1124 (2021).
14. Nightingale, K. Acoustic radiation force impulse (ARFI) imaging: a review. *Curr. Med. Imaging Rev.* **7**, 328–339 (2011).
15. Sigrist, R. M. S., Liau, J., Kaffas, A. E., Chammas, M. C. & Willmann, J. K. Ultrasound elastography: review of techniques and clinical applications. *Theranostics* **7**, 1303–1329 (2017).
16. Genes, I. et al. Ultrasonographic and histopathological features of cervical lymph node metastases. *Rom J. Morphol. Embryol.* **55**, 369–375 (2014).
17. Shiina, T. et al. WFUMB guidelines and recommendations for clinical use of ultrasound elastography: part 1: basic principles and terminology. *Ultrasound Med. Biol.* **41**, 1126–1147 (2015).
18. Habenicht, L. M., Albershardt, T. C., Iritani, B. M. & Ruddell, A. Distinct mechanisms of B and T lymphocyte accumulation generate tumor-draining lymph node hypertrophy. *Oncoimmunology* **5**, e1204505 (2016).
19. Kretschmer, L. et al. The Sentinel node invasion level (SNIL) as a prognostic parameter in melanoma. *Mod. Pathol.* **34**, 1839–1849 (2021).
20. Vassallo, P., Wernecke, K., Roos, N. & Peters, P. E. Differentiation of benign from malignant superficial lymphadenopathy: the role of high-resolution US. *Radiology* **183**, 215–220 (1992).
21. Ariji, Y. et al. Power doppler sonography of cervical lymph nodes in patients with head and neck cancer. *AJNR Am. J. Neuroradiol.* **19**, 303–307 (1998).
22. Meola, M., Ibeas, J., Lasalle, G. & Petrucci, I. Basics for performing a high-quality color doppler sonography of the vascular access. *J. Vasc Access.* **22**, 18–31 (2021).
23. Sun, Y., Wang, W., Mi, C., Zhang, Q. & Zhang, K. Differential diagnosis value of Shear-Wave elastography for superficial enlarged lymph nodes. *Front. Oncol.* **12**, 908085 (2022).
24. Rago, T. et al. Low elasticity of thyroid nodules on ultrasound elastography is correlated with malignancy, degree of fibrosis, and high expression of Galectin-3 and Fibronectin-1. *Thyroid* **27**, 103–110 (2017).
25. Levental, K. R. et al. Matrix crosslinking forces tumor progression by enhancing integrin signaling. *Cell* **139**, 891–906 (2009).
26. Rizwan, A. et al. Metastatic breast cancer cells in lymph nodes increase nodal collagen density. *Sci. Rep.* **5**, 10002 (2015).
27. Guan, Y. et al. A pilot study: N-Staging assessment of shear wave elastrography in small cervical lymph nodes for nasopharyngeal carcinoma. *Front. Oncol.* **10**, 520 (2020).
28. Chae, S. Y., Jung, H. N., Ryoo, I. & Suh, S. Differentiating cervical metastatic lymphadenopathy and lymphoma by shear wave elastography. *Sci. Rep.* **9**, 12396 (2019).
29. Aramaki, N. et al. Drastic morphological and molecular differences between lymph node micrometastatic tumors and macrometastatic tumors of lung adenocarcinoma. *J. Cancer Res. Clin. Oncol.* **142**, 37–46 (2016).
30. Miura, K., Nasu, H. & Yamamoto, S. Scanning acoustic microscopy for characterization of neoplastic and inflammatory lesions of lymph nodes. *Sci. Rep.* **3**, 1255 (2013).
31. Dietrich, C. F. et al. Guidelines and recommendations on the clinical use of liver ultrasound elastography, update 2017 (Short Version). *Ultraschall Med.* **38**, 377–394 (2017).
32. Weiss, L. M. Malley, benign lymphadenopathies. *Mod. Pathol.* **26** (Suppl 1), 88–96 (2013).
33. Luo, C. et al. The value of shear wave elastography in the diagnosis of breast Cancer axillary lymph node metastasis and its correlation with molecular classification of breast masses. *Front. Oncol.* **12**, 846568 (2022).
34. Chami, L. et al. Quantitative and qualitative approach for shear wave elastography in superficial lymph nodes. *Ultrasound Med. Biol.* **47**, 2117–2127 (2021).
35. Asano, S. Granulomatous lymphadenitis. *J. Clin. Exp. Hematop*. **52**, 1–16 (2012).
36. Zaatar, R., Biet, A., Smail, A., Strunski, V. & Page, C. [Cervical lymph node tuberculosis: diagnosis and treatment]. *Ann. Otolaryngol. Chir. Cervicofac.* **126**, 250–255 (2009).
37. Auerbach, A., Schmieg, J. J. & Aguilera, N. S. Pediatric lymphoid and Histiocytic lesions in the head and neck. *Head Neck Pathol.* **15**, 41–58 (2021).
38. Chaouhan, H. S. et al. Necroptosis: A pathogenic negotiator in human diseases. *Int. J. Mol. Sci.* **23**, (2022).
39. Bayramoglu, Z. et al. Diagnostic performances of Superb microvascular imaging, shear wave elastography and shape index in pediatric lymph nodes categorization: a comparative study. *Br. J. Radiol.* **91**, 20180129 (2018).

Acknowledgements

We would like to express our thanks to all of the people who have participated in this research.

Author contributions

XQ is responsible for the design and implementation of research. JC and YD are responsible for data analysis and article writing. JX, WL, GS and HL selected research subjects and operated the US examination. YW is responsible for the implementation of the research, as well as the data collection and analysis. All authors read and approved the final manuscript.

Funding

This work was supported by the Key R&D plan of Hubei Province [grant number 2022BCA050]; the Natural Science Foundation of China [grant number 81901769]; and the Hubei Province health and family planning scientific research project [grant number WJ2023M133].

Declarations

Competing interest
The authors declare no competing interests.

Ethics approval and consent to participate
The study was approved by the Ethics Committee of Union Hospital affiliated to Tongji Medical College of Huazhong University of Science and Technology, and obtained the informed consent of all patients. (Ethics approval ID: UHCT-IEC-SOP-016-03-01)

Additional information
Correspondence and requests for materials should be addressed to Y.W. or X.Q.